



1
2
3
4
5
6
7
8
9
10
11

Extraterrestrial dust as a source of bioavailable Fe for the ocean productivity

Rudraswami. N. Gowda^{1*}, Mayank Pandey¹, Matthew. J. Genge², Dafilgo Fernandes¹

¹CSIR-National Institute of Oceanography, Dona Paula, Goa 403004, India

**²Department of Earth Science and Engineering, Imperial College London, SW7 2AZ,
UK**

***Corresponding author: rudra@nio.org**



12 **Abstract**

13 **Bioavailable Fe is an essential nutrient for phytoplankton that allows organisms to**
14 **flourish and drawdown atmospheric CO₂ affecting global climatic condition. In marine**
15 **locales remote from the continents extraterrestrial-dust provides an important source of**
16 **Fe and thus moderates primary productivity. Here we provide constraints on partitioning**
17 **of extraterrestrial Fe between seawater and sediments from observations of dissolution**
18 **and alteration cosmic spherules recovered from the deepsea sediments and Antarctica.**
19 **Of the ~3,000-6,000t/a extraterrestrial dust that reaches Earth surface, ~2–5% material**
20 **survives in marine sediments whilst the remainder is liberated into seawater. Both**
21 **processes contributes $\sim(3-10)\times 10^{-8}\text{molFe m}^{-2}\text{yr}^{-1}$. Also, Fe contribution due to evaporation**
22 **of survived particle is estimated to be ~10% of Fe contribution to meteoric smoke.**
23 **Changes in extraterrestrial-dust flux vary not only the amount of Fe by up to three orders**
24 **of magnitude, but also the partitioning of Fe between surface and abyssal waters**
25 **depending on entry velocity and evaporation.**

26

27 **Keywords: Iron, Extraterrestrial, Micrometeorites**

28

29

30



31 **1. Introduction**

32

33 Iron (Fe) is the fourth most abundant element in the Earth's crust; nevertheless, it's
34 solubility and accessibility is an essential criterion for bioavailability in isolated regions of the
35 ocean (Johnson, 2001; Shaked et al., 2005; Norman et al., 2014). Bioavailable Fe is an essential
36 micronutrient for the growth and survival of phytoplankton and thus impacts the drawdown of
37 CO₂ by the oceans. It is primarily delivered by aeolian dust from continental interiors to oceans,
38 however, it's failure to reach isolated High Nutrient Low Chlorophyll (HNLC) areas, such as
39 Southern Ocean regions can impact the marine ecosystem and productivity (Jickells et al.,
40 2005; Mahowald et al., 2005). Extraterrestrial dust may have a vital role in rejuvenating the
41 biogeochemistry of the ocean for those areas where the Fe supply from aeolian dust or
42 upwelling is scarce and is not sufficient for active primary productivity (Johnson, 2001; Reiners
43 and Turchyn, 2018).

44

45 The heating of extraterrestrial dust during its atmospheric entry causes Fe to be added
46 to the oceans in two distinct forms: (1) surviving particles, known as micrometeorites (MMs),
47 that reach the Earth's surface (Genge et al., 2008), and (2) meteoritic smoke particles (MSPs)
48 formed by recondensation of evaporated dust in the atmosphere (e.g. Hunten et al., 1980; Lanci
49 et al., 2012). The nature of surviving particles varies considerably with particle size, entry angle
50 and entry velocity that determines their degree of heating (Love and Brownlee, 1993). Those
51 particles with lower entry angle into the atmosphere, however, can survive as partially melted
52 scoriaceous MMs, or at the lowest angles survive without melting (Love and Brownlee, 1991;
53 Rudraswami et al., 2016, 2018). With increasing size the proportion of cosmic spherules in
54 surviving particles increases, whilst unmelted particles are most abundant at sizes of <50 μm
55 (Genge et al., 2008). The precursor material prior to atmospheric entry, which is related to the



56 source parent body, also influences the nature of the surviving MMs, for example, scoriaceous
57 MMs form by partial melting of hydrated fine-grained matrix similar to that of carbonaceous
58 chondrites and derived from C-type asteroids (Taylor et al., 2012; Genge et al., 2017).
59 Extraterrestrial dust entering the atmosphere at high angles are most intensely heated and
60 experience partial to complete evaporation (Love and Brownlee, 1991). The compositions of
61 cosmic spherules testify to this process and show depletions in volatile and moderately volatile
62 elements relative to chondrites. Ultimately this evaporated matter recondenses as nanometric
63 smokes and settle to the Earth's surface (Lanci et al., 2012). Both smoke and surviving MMs
64 are added to the oceans.

65

66 The role of extraterrestrial dust in the supply of Fe to the oceans has three significant
67 outstanding uncertainties: (1) the average Fe content of incident dust, (2) the proportion of Fe
68 delivered by surviving MMs compared to MSPs, and (3) the relative proportion of
69 extraterrestrial Fe that is sequestered by seawater compared to that buried to ocean sediments.
70 The current work presents data on the abundances, compositions and mineralogies of
71 extraterrestrial dust recovered from deep sea sediments to address these questions. The absolute
72 flux of extraterrestrial dust is also discussed through comparisons to other micrometeorite
73 collections and suggests of flux of extraterrestrial Fe of up to $\sim 10^{-6}$ mol Fe m⁻² yr⁻¹.

74

75 **2. Samples and Analytical Techniques**

76

77 The present work has compiled micrometeorites from deep-sea sediment of central
78 Indian Ocean and Antarctica. The deep-sea sediments collected by using surficial grab sampler
79 (size 50×50 cm (length × breadth) from the ocean depth of ~5000 m. The second collection
80 from Antarctica, Maitri station was undertaken by ice melting and sieving the melted water



81 using ~50 μm mesh. The particulars of the sampling process from the deep-sea collection have
82 been described in detail by Prasad et al. (2013) and Rudraswami et al. (2012, 2018). The
83 micrometeorites from both these collections were mounted on epoxy for polishing to uncover
84 the interior surface, which was carbon coated for electron microscopy studies using scanning
85 electron microscope (SEM, JEOL JSM-IT3001V SEM with an OXFORD INCA Energy
86 Dispersive Spectrometer detector National Institute of Oceanography, Goa) and electron Probe
87 Micro Analyzer (EPMA, Cameca SX5). The back-scattered electron (BSE) image was obtained
88 to classify the texture and for identification of the phases.

89

90 We have identified 5699 particles but have discarded G-type (87) and I-type (384)
91 particles and focused our studies on S-type particles (5228). The S-type carefully chosen for
92 the studies are as follows: scoriaceous: 220, relict-bearing: 250, porphyritic: 1710, barred:
93 1818, cryptocrystalline: 610, and glass: 620. All the particles are analyzed for minor and major
94 chemical composition (Na, Mg, Si, Al, P, K, Ca, Ti, Cr, Fe, Ni, Mn) using electron microprobe
95 to obtain bulk chemical composition which are provided in Supplementary file A. Analyses on
96 each particle varied from ~10 to 20 spots having a beam size of ~2–5 μm with gaps between
97 each point such that the entire particle was covered representing true bulk composition. The
98 specifics related to the electron microscopy analyses technique is discussed elsewhere
99 (Rudraswami et al., 2011; Rudraswami et al. 2012). These studies are focused on particle sizes
100 that deliver the mass peak of the ET matter to Earth.

101

102 **3. Results and Discussion**

103 **3.1. The type of micrometeorite and average Fe-content**

104



1205 The types of MMs recovered on Earth vary significantly with particle size. At diameters
1206 of ~200 μm studies of unmelted MMs recovered from Antarctic ice reveal that the majority are
1207 dominated by materials with fine-grained hydrated precursors similar to the CI and CM
1208 chondrites, with a smaller proportion of CR materials (Genge et al., 2008; Taylor et al., 2012).
1209 Crystalline MMs present are dominated by olivine, pyroxene and glass. These particles are
1210 thought to be fragments of chondrules from chondritic parent bodies and include particles from
1211 ordinary chondrites (OCs; Genge, 2008; Prasad et al., 2015). Although unmelted particles
1212 represent a small fraction of MMs in this size range, they are representative of the flux since
1213 they survive by virtue of their low entry angles, thus cosmic spherules will have the same
1214 sources. Using the bulk compositions of different parent bodies the Fe contribution from each
1215 parental type of MM that is calculated is shown in Fig. 1. We have used various composition
1216 of chondritic Fe content which is provided in Hutchison (2004), and Johnson (2001) formula
1217 to calculate the total Fe for various chondrites to generate the Table 1. The formula is as
1218 follows: Total bioavailable input to ocean = [(Extraterrestrial Flux) \times 0.9 (considering 90%
1219 ablation) \times 0.7 (70% area of Earth is covered by ocean) \times (weight percent of iron of various
1220 chondrites)] / [area of ocean \times molar mass of Fe]. The area of global ocean considered for this
1221 study is $\sim 3.62 \times 10^8 \text{ km}^2$. We have incorporated 90% ablation for ground based collection
1222 technique to calculate the total flux before atmospheric entry. This 90% ablation is based on
1223 Taylor et al. (1998) where they have considered Love and Brownlee (1993) flux data from
1224 experiments done on Long Duration Exposure Facility (LDEF) at an orbital altitude of ~300–
1225 400 km.

1226

1227 Observations of large MMs ($>300 \mu\text{m}$) from the Transantarctic mountains suggest that
1228 the contribution of ordinary chondrites becomes higher (~30%) at large sizes (Cordier et al.,
1229 2011; Van Ginneken et al., 2017) will increase the average Fe content. Since particle abundance



130 decreases exponentially with size, however, the increase in the average will be small. Small
131 MMs are dominated by hydrous particles similar to carbonaceous chondrites, but contain ~40%
132 carbon-rich, porous cometary particles (Noguchi et al., 2015). The abundance of Fe within
133 cometary porous particles is lower than in chondrites since it is diluted by abundant
134 carbonaceous matter (>30%). The increase in average Fe owing to large OC particles is,
135 therefore, offset by its lower content in small cometary grains. The parent body abundances
136 amongst Indian Ocean cosmic spherules, therefore, give a good estimate for the average Fe
137 abundance of the ET flux prior to atmospheric entry.

138

139 **3.2. Relative importance of smokes and micrometeorites**

140

141 Numerical models of atmospheric entry suggest that ~90% of the Extraterrestrial dust
142 mass flux is lost to evaporation during atmospheric entry (Love and Brownlee, 1993). MMs
143 collected from Antarctic snow at the South Pole Water Well provide a means of evaluating the
144 proportion of mass lost to evaporation (Taylor et al., 1998). Different researchers using various
145 collection techniques have arrived at different flux rate. It was estimated based on courting
146 statistics by Taylor et al. (1998) from South Pole Water Well (SPWW) that ~3000 tonnes per
147 annum survive the heating during atmospheric entry and reach the Earth surface indicating that
148 more than ~90% that get ablated does not make it to Earth's surface. This estimate of particles
149 reaching the Earth surface is lower than that estimated by Yada et al. (2004) who has coupled
150 the handpicking of micrometeorites and noble gas measurement from the residue, and has
151 indicated a range of 11000–16000 tonnes per annum as the extraterrestrial material reaching
152 the Earth surface. However, Yada et al. (2004) based only on handpicked particle count has
153 shown ~5000–7000 tonnes per annum. This is much higher than those estimated by previous
154 researchers, probably one of the reason is the smaller sieved size used by Yada et al. (2004).



155 Nevertheless, the micrometeorites from deep-sea sediments are much lower than Antarctica
156 (Brownlee et al., 1997; Prasad et al., 2013). Measurements of micro-impact craters on the
157 LDEF satellite provide arguably the most accurate observational evidence for the total flux of
158 Extraterrestrial dust prior to atmospheric entry at $40,000 \text{ t a}^{-1}$ (Love and Brownlee, 1993). The
159 total fraction of evaporated material is thus 80–90% with a most likely value of ~90% similar
160 to that predicted by models of entry heating.

161

162 Partial evaporation must also be considered when evaluating the proportion of Fe
163 liberated by evaporation and the formation of smokes. The composition of 5228 deepsea and
164 Antarctica spherules analysed in the current study is shown in Fig. 2 (data in supplementary
165 file A) based on their texture classification which suggests preferential loss of Fe compared to
166 more refractory elements such as Al, Ca, Mg, and Si. An average Fe content of ~20 wt% is
167 retained in Indian Ocean spherules. Since these particles are the surviving remnants of
168 evaporation, the fractionation of Fe during entry heating can be estimated by comparison to the
169 predicted precursor average Fe content of ~23% (carbonaceous and ordinary chondrites). This
170 suggests that MSPs that contribute $\sim 2 \text{ t d}^{-1}$ (Hervig et al., 2017) are enriched in Fe by
171 comparison to their precursor compositions by a factor of 3–7 times based on the ground based
172 collection techniques (Taylor et al., 1998; Yada et al., 2004). Hence, the overall Fe contribution
173 based on particle chemical analyses is estimated be $\sim 0.2\text{--}0.5 \text{ t d}^{-1}$ which is ~10% of MSPs
174 contribution. Dhomse et al. (2013) studied the transport of MSPs and their deposition to the
175 earth's surface and predicted preferential deposition occurs at mid-latitudes by a factor of ~10
176 compared to other locales. Nevertheless, Lanci et al. (2012) showed that nanometer size
177 supramagnetic iron exists within polar ice indicating that the recondensed evaporated portion
178 of incoming ET material does reach the Earth's surface at all latitudes.

179



180 **3.3. Burial of extraterrestrial Fe in Ocean sediments**

181

182 Many previous researchers related to the topic of “Fe source to Ocean by extraterrestrial
183 input” has focused only on the total material that is hit above the Earth’s surface ignoring the
184 contribution from the micrometeorites that fall on Earth surface. The sample that is retained
185 from the Earth surface have evaporated nearly ~10 to 80% of their original mass, besides,
186 etching that it undergoes in the ocean contributing effectively to marine biogeochemistry. Most
187 of the preserved sample from the ocean are etched compared to inside portion as represented
188 in Figure 1. Ignoring the size of the spherule, the percent of spherule etched out in different
189 types of spherules varies given the age (~0–50,000 years) of the sediment from which the
190 sample is collected (Prasad et al., 2013). The etching is commonly observed in barred spherules
191 due to hydration. The more the time spherule spent in seawater, the more it gets etched out.
192 The sample once gets settled in the sediments the chances of etching diminishes. All the
193 spherules show varying levels of etching considering their large range in terrestrial ages,
194 except, the barred spherules that show maximum etching among all textural types. The etching
195 phenomena is commonly seen in any collection, whether it is Antarctica or deep-sea sediments,
196 while it is dominant in later due to large residence time and harsh condition of ocean. The glass
197 spherules have shown minimum alteration compared to its counterpart due low porosity, and
198 highly melted during atmospheric entry. Papanastassiou et al. (1983) observed no chemical
199 alteration in measured $^{87}\text{Sr}/^{86}\text{Sr}$ ratios and the Sr concentration in the analyzed deep-sea
200 spherules have typical chondritic range suggesting that they have not exchanged Sr with
201 seawater. The Rb depletion in spherules is related to volatilization during atmospheric entry
202 and has not related to weathering in seawater. They concluded that the $^{87}\text{Sr}/^{86}\text{Sr}$ in deep-sea
203 spherules is consistent with origin from chondritic composition meteoroids and appears to
204 exclude most other possible terrestrial sources. Also extensive study of nearly ~300 spherules



205 done by Bate et al. (1986) drawn conclusion that the average Mg/Si, Al/Si and Ca/Si ratios of
206 the deep-sea spherule has not changed with time scale in spite of etching.

207

208 The abundance of deep sea spherules collected in the Indian Ocean provides a direct
209 measurement of the proportion of ET Fe buried within ocean sediments. The deficit between
210 the flux of MMs retained in sediments and the flux at the top of the atmosphere relates to the
211 mass lost to evaporation, plus the mass of MMs dissolved into seawater. The mass lost to
212 evaporation was suggested above to be ~90%. Values of the spherule flux of $\sim 160 \text{ t a}^{-1}$ from
213 the Indian Ocean collection (Prasad et al., 2013), therefore, suggest the mass of Fe released by
214 dissolution into seawater is ~5–10% of the total incoming Fe flux (>90% of MMs destroyed
215 by dissolution). The degree of dissolution of MMs through alteration in seawater can be
216 independently confirmed by the relative abundance of I-type cosmic spherules. These particles
217 form by atmospheric entry and oxidation of metal grains to magnetite (Fe_3O_4) and wustite
218 (FeO). Both these minerals are highly resistant to aqueous alteration compared with silicates.
219 The relative abundance of I-types to S-type (silicate) spherules, therefore, gives a measure of
220 proportion of S-types destroyed by dissolution. The abundance of I-types in the Indian Ocean
221 collection is ~5% whilst that in the South Pole Water Well is ~1% suggesting the loss of ~80%
222 of S-type spherules by dissolution in the ocean, broadly consistent with the fraction predicted
223 from the over-all spherule abundance.

224

225 Although ~80–90% of deep sea spherules can be inferred to have been destroyed by
226 dissolution, surviving particles also exhibit evidence for significant etching which varies from
227 20 to 90% by volume (Fig. 3). S-type cosmic spherules often show the removal of interstitial
228 glass between crystals of olivine with etching concentrated in external rims (Fig. 3). Glass in
229 these particles is Fe-rich in comparison to olivine, which is usually Mg-rich, consequently



230 etching causes loss of Fe. The rough estimate based on Taylor et al. (1998) or Yada et al.
231 (2004) flux calculation indicate that $\sim 3,000\text{--}16,000\text{ t a}^{-1}$ of ET material get dissolved bring
232 $\sim 25\text{--}30\%$ of Fe from total flux depending on different types of precursors. This will add at
233 least $\sim (3\text{--}10)\times 10^{-8}\text{ mol Fe m}^{-2}\text{ yr}^{-1}$. However, particles etching of $\sim 20\text{--}90\%$ in seawater
234 contribute few percent to the above value.

235

236 **4. Implications**

237

238 Data from the Indian Ocean collection of deep sea spherules suggests that slightly more
239 than 90% of Fe within extraterrestrial dust incident on the atmosphere is lost from particles
240 during evaporation and delivered to the ocean as recondensed MSPs. Amongst the 10% of
241 extraterrestrial dust that survives atmospheric entry $>90\%$ of the initial flux of Fe is liberated
242 by dissolution of MMs in seawater, with 2–5% buried within deep sea sediments and thus not
243 bioavailable. Given a measured flux of $40,000\text{ t a}^{-1}$ this suggests an average $3\times 10^{-7}\text{ mol Fe m}^{-2}$
244 yr^{-1} of Fe delivered to the oceans. Some simulations of the flux of dust delivered to the Earth,
245 based on its orbital evolution, however, suggest a maximum of $\sim 10^5\text{ t a}^{-1}$ (Nesvorný et al.,
246 2010) and approximately double the Fe flux. Estimates of the flux of terrestrial dust to the
247 Southern Ocean give a total mass of $30\times 10^{-6}\text{ mol Fe m}^{-2}\text{ yr}^{-1}$ (Lancelot et al., 2009), however,
248 silicic volcanic dust and wind-blown clastic grains dominated by quartz are both Fe-poor.
249 Furthermore, Fe in such terrestrial dust particles is present as Fe oxides that are relatively
250 resistant to dissolution in seawater. The soluble fraction is likely to be $<1\%$. The ET Fe flux is,
251 therefore, likely to be similar to that from terrestrial sources. In the Southern Ocean
252 concentration of MSPs is also increased by a factor of 10 and is likely exceed terrestrial sources
253 and dominate primary production of phytoplankton (Dhomse et al., 2013). Elsewhere MSP are



254 less abundant and Fe from surviving particles represent a larger fraction (~20%) of
255 extraterrestrial Fe.

256

257 The nature of ET inputs of Fe to the oceans, however, are also crucially important.
258 Meteoritic smokes represent the largest input to the oceans and are dominated by nanometric
259 dust (Lanci et al., 2012), which are likely to be readily soluble owing to their high surface area
260 to mass ratio. Smokes are added directly to the ocean surface and rapidly release their Fe within
261 the photic zone. This Fe is, therefore, immediately available to phytoplankton. At low
262 sedimentation rates of a few microns per year on parts of the abyssal plain of settled particles
263 are exposed to seawater where Fe get leached out by dissolution of MMs at abyssal depths.
264 The Fe derived by dissolution of MMs, therefore, is not immediately available to phytoplankton
265 but is stored at depth until upwelling currents bring it to the surface. In areas distal to the
266 continents, such as isolated islands and seamounts, and the intertropical convergence zone,
267 extraterrestrial Fe may impact primary production.

268

269 Currently the importance of extraterrestrial Fe in primary production is likely to be
270 localised within those areas with the lowest influx of terrestrial dust. The ET flux of dust,
271 however, has been elevated at times in the Earth's past such as in the Ordovician (Schmitz et
272 al., 2019) and at the end of the Eocene (Meier et al., 2016), with increases in flux up to 2–3
273 orders of magnitude. During these periods extraterrestrial Fe delivered to the oceans may have
274 dominated primary production more widely and thus affected global CO₂ budget. This
275 mechanism, together with atmospheric dust load, has already been suggested as an origin for
276 the end Ordovician glaciation (Schmitz et al., 2019). Evidence also exists for periodic changes
277 in the ET flux the eccentricity variations in the Earth's orbit. Periods of higher entry velocity
278 will enhance evaporation of dust and delivery of Fe to the photic zone of the ocean, whilst



279 lower entry velocity will increase Fe delivered to abyssal waters that replenish the surface by
280 subsequent vertical mixing. The velocity distribution of extraterrestrial dust, therefore, will
281 influence the consequences of the delivery of extraterrestrial Fe to Earth.

282

283 **5. Conclusion**

284

285 Data from the abundance, composition and textures of deep sea spherules allow the first
286 assessment partitioning of extraterrestrial Fe between MSPs, surviving micrometeorites,
287 marine sediments and ocean water. The abundance of extraterrestrial Fe liberated by
288 evaporation is suggested to be enhanced owing to the effects of partial evaporation and forms
289 part of the component delivered to the oceans as MSPs. This material dominates the flux of
290 extraterrestrial Fe delivered to the oceans and is dissolved in the photic zone of the oceans
291 where it directly impacts primary productivity. Surviving MMs in contrast undergo 80–90%
292 dissolution in the oceans and their Fe is delivered to abyssal depths. Upwelling of seawater
293 from depth allows this extraterrestrial Fe to contribute to primary productivity. At present
294 extraterrestrial Fe is important in areas where the supply of terrestrial dust is low, such as in
295 the Southern Oceans, however, during periods in which ET flux is enhanced it is likely to have
296 a wider-spread contribution to productivity and thus CO₂ drawdown by the oceans affecting
297 global climate.



298 **Data availability.** The supporting data (supplementary A) related to this article is available at
299 Dryad Dataset (<https://datadryad.org/stash/dataset/doi:10.5061/dryad.zcrjdfn7t>).

300

301 **Author contributions.** NGR is involved in collecting micrometeorites, project funding,
302 formulating the research objective. MP is involved in compilation of data and preparation of
303 the manuscript. DF is involved in collection and analysis of data. MJG is involved in
304 preparation of the manuscript.

305

306 **Competing interests.** The authors declare that they have no conflict of interest.

307

308 **Acknowledgements.** We thank Areef and Vijay Khedekar for electron microscopy work. This
309 work was supported by the PMN, GEOSINK and PLANEX project. The supporting data
310 (supplementary A) related to this article is available at Dryad Dataset
311 (<https://datadryad.org/stash/dataset/doi:10.5061/dryad.zcrjdfn7t>).

312

313 **Financial support.** This work was supported by the PMN, GEOSINK and PLANEX project.



314 **REFERENCES**

315 Bates, B. A.: The elemental composition of stony extraterrestrial particles from the ocean
316 floor, PhD thesis, 199 pp., University of Washington, Seattle, WA, 1986.

317 Brownlee, D.E., Bates, B. A., and Schramm, L.: Elemental composition of stony cosmic
318 spherules, *Meteoritics & Planetary Science*, 32, 157–175, 1997.

319 Cordier, C., Folco, L., Suavet C., Sonzogni, C., and Rochette, P.: Major, trace element and
320 oxygen isotope study of glass cosmic spherules of chondritic composition: the record of
321 their source material and atmospheric entry heating, *Geochim. Cosmochim. Acta*, 75,
322 5203–5218, 2011.

323 Dhomse S. S., Saunders R. W., Tian W., Chipperfield, M. P., and Plane, J. M. C.:
324 Plutonium-238 observations as a test of modeled transport and surface deposition of
325 meteoric smoke particles, *Geophysical research letters*, 40, 4454-4458, 2013.

326 Dohnanyi, J.S.: Interplanetary objects in review: Statistics of their masses and dynamics,
327 *Icarus*, 17, 1-48, 1972.

328 Genge M. J., Engrand C., Gounelle, M., and Taylor, S.: The classification of
329 micrometeorites. *Meteorit. Planet. Sci.*, 43, 497– 515, 2008.

330 Genge, M. J., Suttle, M. J., and Van Ginneken, M.: Thermal shock fragmentation of Mg
331 silicates within scoriaceous micrometeorites reveal hydrated asteroidal sources, *Geology*,
332 45, 891-894, 2017.

333 Genge, M. J.: Koronis asteroid dust within Antarctic ice, *Geology*, 36 (9), 687-690, 2008.

334 Genge, M.J., Suttle, Martin., & van Ginneken, M.: Thermal shock fragmentation of Mg
335 silicates within scoriaceous micrometeorites reveal hydrated asteroidal sources, *Geology*,
336 45, 891-894, 2017.

337 Hammer, C., and M, Maurette.: "Micrometeorite flux on the melt zone of the West
338 Greenland ice sheet", *Meteoritics and Planetary Science Supplement*, 31, 1996.

339 Hervig, M. E., Brooke, J. S. A., Feng, W., Bardeen, C. G., and Plane, J. M. C.: Constraints
340 on meteoric smoke composition and meteoric influx using SOFIE observations with
341 models, *Journal of Geophysical Research: Atmospheres*, 122, 13495– 13505, 2017.



- 342 Hunten, D. M., Turco, R. P., & Toon, O. B.: Smoke and dust particles of meteoric origin
343 in the mesosphere and stratosphere, *J. Atmos. Sci*, 37, 1342– 1357, 1980.
- 344 Hutchison, R.: *Meteorites: A Petrologic, Chemical and Isotopic Synthesis*, Cambridge
345 Univ., Cambridge, 2004.
- 346 Jickells, T. D., An, Z. S., Andersen, K. K., Baker, A. R., Bergametti, G., Brooks, N., Cao,
347 J. J., Boyd, P. W., Duce, R. A., Hunter, K. A., Kawahata, H., Kubilay, N., Laroche, J., Liss,
348 P. S., Mahowald, N., Prospero, J. M., Ridgwell, A. J., Tegen, I. & Torres, R.: Global iron
349 connections between desert dust, ocean biogeochemistry, and climate, *Science*, 308, 67-71,
350 2005.
- 351 Johnson, K. S.: Iron supply and demand in the upper ocean: Is extraterrestrial dust a
352 significant source of bioavailable iron?, *Global Biogeochem. Cycles*, 15(1), 61– 63, 2001.
- 353 Lancelot, C., deMontety, A., Goosse, H., Becquevort, S., Schoemann, V., Pasquer, B.,
354 and Vancoppenolle, M.: Spatial distribution of the iron supply to phytoplankton in the
355 Southern Ocean: A model study, *Biogeosciences*, 6, 2861–2878, 2009.
- 356 Lanci, L., Delmonte, B., Kent, D., Maggi, V., Biscaye, P. E., and Petit, J. R.: Magnetization
357 of polar ice: A measurement of terrestrial dust and extraterrestrial fallout, *Quat. Sci. Rev.*,
358 33, 20–31, 2012.
- 359 Love, S. G. & Brownlee, D. E.: A Direct Measurement of the Terrestrial Mass Accretion
360 Rate of Cosmic Dust, *Science*, 262, 550–553, 1993.
- 361 Love, S. G., & Brownlee, D. E.: Heating and thermal transformation of micrometeoroids
362 entering the Earth’s atmosphere. *Icarus*, 89, 26–43, 1991.
- 363 Mahowald, N. M., Baker, A. R., Bergametti, G., Brooks, N., Duce, R. A., Jickells, T. D.,
364 Kubilay, N., Prospero, J. M., and Tegen, I.: Atmospheric global dust cycle and iron inputs
365 to the ocean, *Global Biogeochem. Cycles*, 19, GB4025, 2005.
- 366 Maurette M., Jéhanno C., Robin E., and Hammer C.: Characteristics and mass distribution
367 of extraterrestrial dust from the Greenland ice cap, *Nature*, 328, 699–702, 1987.
- 368 Meier, M. M. M., Maden, C., and Busemann, H.: Constraining the Age of the Veritas
369 Asteroid Break-Up Event with Helium-3 from the Tortonian Monte Dei Corvi Section in
370 Italy, 79th Annual Meeting of the Meteoritical Society, Abstract, 6288, 2016.



- 371 Murrell, M. T., Davis, P. A., Nishiizumi, K., & Millard, H. T.: Deep sea spherules from
372 Pacific clay: Mass distribution and influx rate, *Geochim. Cosmochim. Acta*, 44, 2067–
373 2074, 1980.
- 374 Nesvorný, D., Jenniskens, P., Levison, H. F., Bottke, W. F., Vokrouhlický, D., and
375 Gounelle, M.: Cometary origin of the zodiacal cloud and carbonaceous micrometeorites:
376 Implications for hot debris disks, *The Astrophysical Journal*, 713(2), 816, 2010.
- 377 Noguchi, T., Ohashi, N., Tsujimoto, S., Mitsunari, T., Bradley, J. P., Nakamura, T., Toh,
378 S., Stephan, T., Iwata, N., and Imae, N.: Cometary dust in Antarctic ice and snow: past and
379 present chondritic porous micrometeorites preserved on the Earth's surface, *Earth and
380 Planetary Science Letters*, 410, 1–11, 2015.
- 381 Norman, L., Cabanesa, D. J., Blanco-Ameijeiras, S., Moisset, S. A., and Hassler, C. S.: Iron
382 biogeochemistry in aquatic systems: From source to bioavailability, *CHIMIA International
383 Journal for Chemistry*, 68 (11), 764-771, 2014.
- 384 Papanastassiou, D. A., Wasserburg, G. I., and Brownlee, D. E.: Chemical and isotopic
385 study of extraterrestrial particles from the ocean floor, *Earth and Planetary Science
386 Letters*, 64, 341–355, 1983.
- 387 Peng, H., and Lui, Z.: Measurement of the annual flux of cosmic dust in deep-sea
388 sediments, *Meteorit. Planet. Sci.*, 24, 315H, 1989.
- 389 Peucker-Ehrenbrink, B., & Ravizza, G.: The effects of sampling artifacts on cosmic dust
390 flux estimates: A reevaluation of nonvolatile tracers (Os, Ir), *Geochim. Cosmochim. Acta*,
391 64, 1965–1970, 2000.
- 392 Plane, J.: Cosmic Dust in the Earth's Atmosphere, *Chemical Society reviews*, 41, 6507-
393 6518, 2012.
- 394 Prasad M. S., Rudraswami N. G., & Panda, D. K.: Micrometeorite flux on earth during the
395 last ~50,000 years, *J. Geophys. Res.*, 118, 2381–2399, 2013.
- 396 Prasad, M.S., Rudraswami, N.G., De Araujo, A., Babu, E.V.S.S.K. and Vijaya Kumar, T.
397 Ordinary chondritic micrometeorites from the Indian Ocean, *Meteorit. Planet. Sci.*, 50,
398 1013-1031, 2015.



- 399 Raiswell, R., Benning, L. C., Tranter, M., & Tulaczyk, S.: Bioavailable iron in the Southern
400 Ocean: the significance of the iceberg conveyor belt, *Geochemical Transactions*, 7, 1-9,
401 2008.
- 402 Reiners, P. W., & Turchyn, A. V. Extraterrestrial dust, the marine lithologic record, and
403 global biogeochemical cycles, *Geology*, 46(10), 863-866. (2018).
- 404 Rudraswami, N. G., Prasad, M. S., Babu, E. V. S. S. K., Kumar, T. V., Feng, W., and Plane,
405 J. M. C.: Fractionation and fragmentation of glass cosmic spherules during atmospheric
406 entry, *Geochimica et Cosmochimica Acta*, 99, 110–127, 2012.
- 407 Rudraswami, N. G., Prasad, M. S., Dey, S., Plane, J. M. C., Feng, W., Carrillo-Sanchez, J.
408 D., and Fernandes, D.: Ablation and chemical alteration of cosmic dust particles during
409 entry into the earth's atmosphere, *The Astrophysical Journal Supplement Series*, 227(2),
410 14, 2016.
- 411 Rudraswami, N. G., Shyam Prasad, M., Nagashima, K., and Jones, R. H.: Oxygen isotopic
412 composition of relict olivine grains in cosmic spherules: Links to chondrules from
413 carbonaceous chondrites, *Geochimica et Cosmochimica Acta*, 164, 53-70, 2015.
- 414 Rudraswami, N.G., Fernandes, D., Naik, A.K., Shyam Prasad, M., Carrillo-Sánchez,
415 J.D., Plane, J.M.C., Feng, W., and Taylor, S.: Selective Disparity of Ordinary Chondritic
416 Precursors in Micrometeorite Flux, *The Astrophysical Journal*, 853, 2018.
- 417 Saunders, R. W., and Plane, J. M.C.: A laboratory study of meteor smoke analogues:
418 Composition, optical properties and growth kinetics, *Journal of Atmospheric and Solar-
419 Terrestrial Physics*, 68, 2182-2202, 2006.
- 420 Schmitz B., Farley K. A., Goderis S., Heck P. R., Bergstrom S. M., Boschi S., Claeys P.,
421 Debaille V., Dronov A., van Ginneken M., Harper D. A. T., Iqbal F., Friberg J., Liao S.,
422 Martin E., Meier M. M., Peucker-Ehrenbrink B., Soens B., Wieler R., and Terfelt, F.: An
423 extraterrestrial trigger for the mid-Ordovician ice age: Dust from the breakup of the L-
424 chondrite parent body, *Science Advances*, 5, 9, eaax4184, 2019.
- 425 Shaked, Y., Kustka, A. B., & Morel, F. M.: A general kinetic model for iron acquisition by
426 eukaryotic phytoplankton, *Limnology and Oceanography*, 50(3), 872-882, 2005.



- 427 Takayanagi, M., & Ozima, M.: Temporal variation of He³/He⁴ ratio recorded in deep-sea
428 sediment cores, *Journal of Geophysical Research*, 921, 12531-12538, 1987.
- 429 Taylor S., Lever, J. H., and Harvey, R. P.: Accretion rate of cosmic spherules measured at
430 the South Pole, *Nature*, 392, 899–903, 1998.
- 431 Taylor, S., Matrajt, G., and Guan, Y.: Fine-grained precursors dominate the micrometeorite
432 flux, *Meteoritics & Planetary Science*, 47, 550 - 564, 2012.
- 433 Van Ginneken, M., Gattacceca, J., Rochette, P., Sonzogni, C., Alexandre, A., and Genge,
434 M.J.: The parent body controls on cosmic spherule texture: Evidence from the oxygen
435 isotope composition of large micrometeorites, *Geochimica et Cosmochimica Acta*, 212,
436 196-210, 2017.
- 437 Yada T., Nakamura T., Takaoka N., Noguchi T., Terada K., Yano H., Nakazawa, T., and
438 Kojima, H.: The global accretion rate of extraterrestrial materials in the last glacial period
439 estimated from the abundance of micrometeorites in Antarctic glacier ice, *Earth Planets
440 Space*, 56, 67–79, 2004.
- 441 Yiou, F., G.M. Raisbeck, & C. Jehanno.: The micrometeorite flux to the Earth, during the
442 last ~200,000 years as deduced from cosmic spherule concentration in Antarctic ice cores,
443 *Meteoritics.*, 26, 412, 1991.
- 444
- 445
- 446



447 **FIGURE CAPTIONS**

448 **Figure 1.**

449

450 Evaluating the contribution of iron from various extraterrestrial chondritic precursors having
451 different Fe content and flux rate estimated by various researchers adopting different
452 methodologies (Table 1). The estimate are done by assuming 90% ablation for the calculated
453 flux by various researchers. It can be seen that Yada et al. (2004) flux shown huge contribution
454 due top more flux reported by them in their collection, while on the other hand the deep-sea
455 collection has lower estimate as a large fraction get etched out in seawater. The bulk Fe content
456 of various chondrites is given by Hutchison (2004).

457

458 **Figure 2.**

459 The plot of major element Fe versus Si and Mg for different type of cosmic spherules, namely,
460 scoriaceous (220), relict-bearing (250), porphyritic (1710), barred (1818), cryptocrystalline
461 (610), and glass (620), respectively.

462

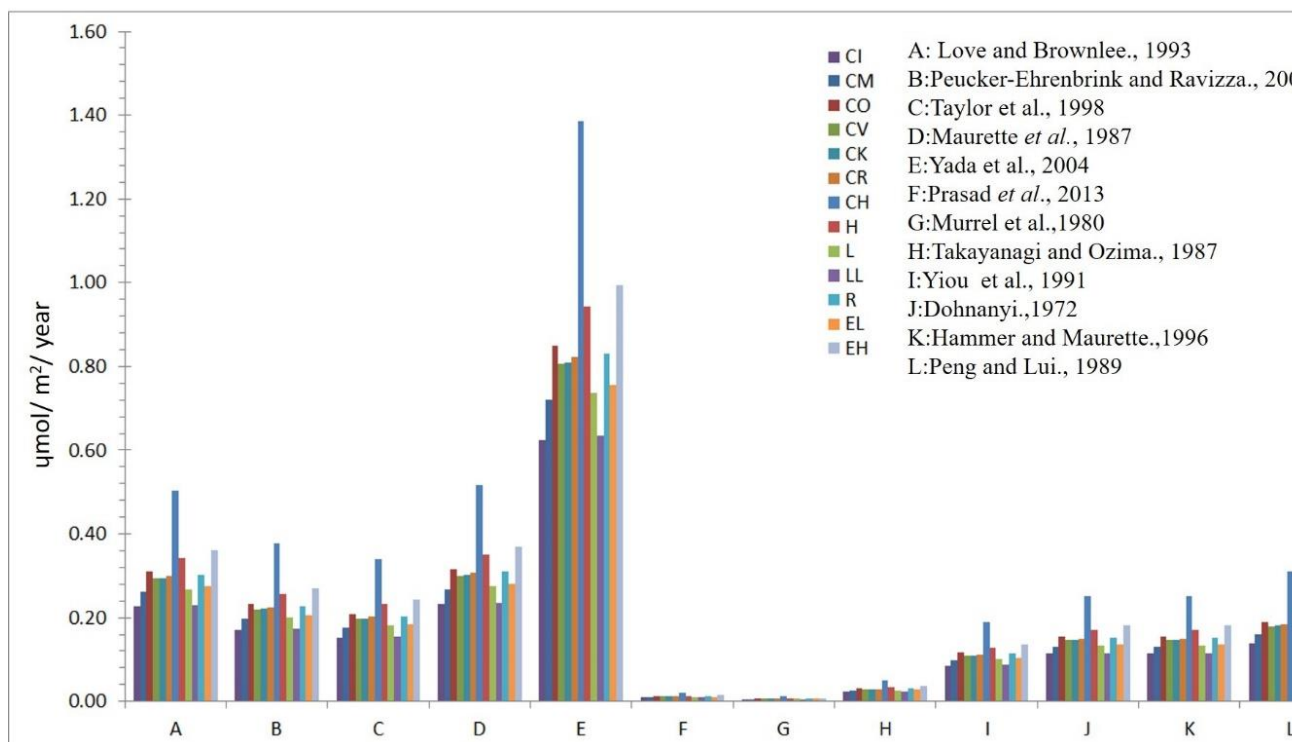
463 **Figure 3.**

464 Back-scattered electron images of the cosmic spherules that have various level of etching
465 collected from deep sea sediments of Indian Ocean.

466



Fig. 1



467

468

469

470

471

472

473

474

475

476

477



478

Fig. 2

479

480

481

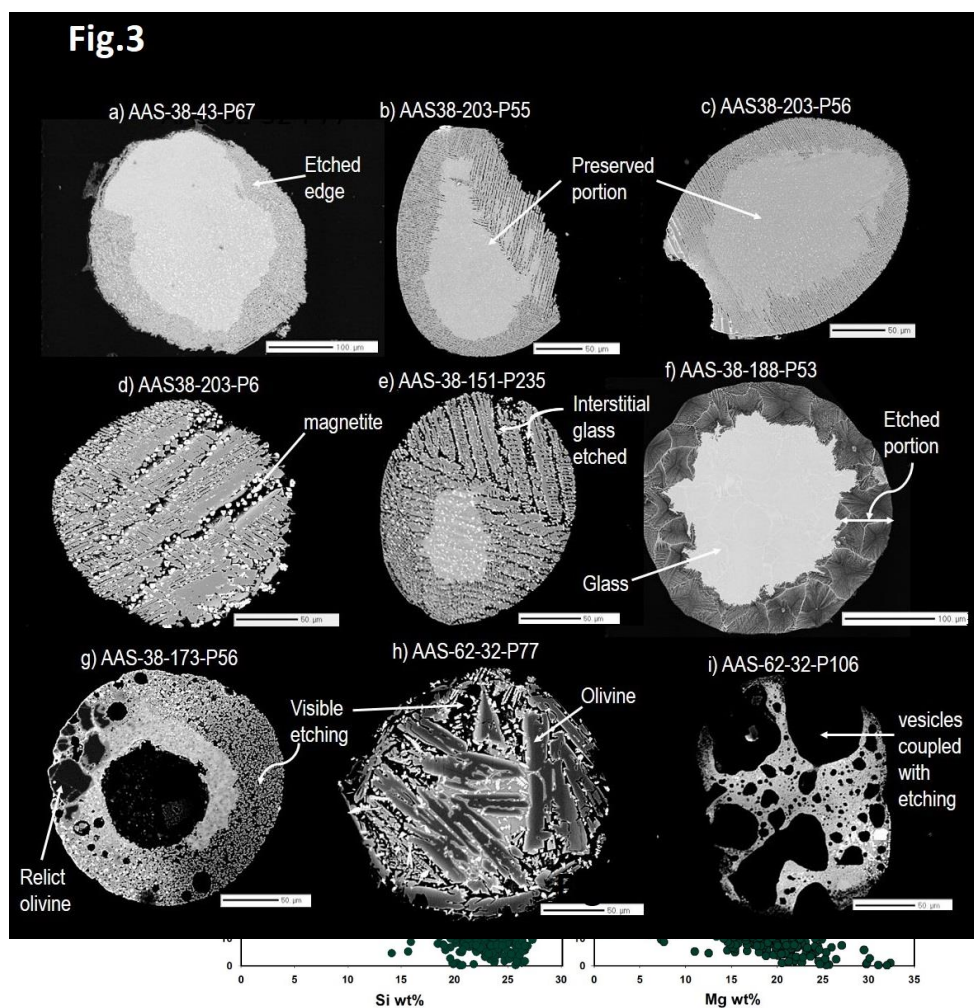
482

483

484

485

486





487 Table 1. The total Fe input to ocean based on different type of chondrites has been calculated using data from Hutchison (2004) and formula based
 488 on Johnson (2001). The ablation of MMs during entry is considered to be ~90% based on Taylor et al. (1998) and Love and Brownlee (1993). The
 489 values in the table are in $\mu\text{mol Fe m}^{-2}\text{yr}^{-1}$.

	Total Fe for CI	Total Fe for CM	Total Fe for CO	Total Fe for CV	Total Fe for CK	Total Fe for CR	Total Fe for CH	Total Fe for H	Total Fe for L	Total Fe for LL	Total Fe for R	Total Fe for EL	Total Fe for EH	
A	0.23	0.26	0.31	0.29	0.29	0.30	0.50	0.34	0.27	0.23	0.30	0.27	0.36	Love and Brownlee, 1993
B	0.17	0.20	0.23	0.22	0.22	0.22	0.38	0.26	0.20	0.17	0.23	0.21	0.27	Peucker-Ehrenbrink and Ravizza, 2000
C	0.15	0.18	0.21	0.20	0.20	0.20	0.34	0.23	0.18	0.16	0.20	0.19	0.24	Taylor et al., 1998
D	0.23	0.27	0.32	0.30	0.30	0.31	0.52	0.35	0.27	0.24	0.31	0.28	0.37	Maurette <i>et al.</i> , 1987
E	0.62	0.72	0.85	0.81	0.81	0.82	1.38	0.94	0.74	0.63	0.83	0.75	0.99	Yada <i>et al.</i> 2004
F	0.01	0.01	0.01	0.01	0.01	0.01	0.02	0.01	0.01	0.01	0.01	0.01	0.01	Prasad <i>et al.</i> 2013
G	0.01	0.01	0.01	0.01	0.01	0.01	0.01	0.01	0.01	0.01	0.01	0.01	0.01	Murrel <i>et al.</i> 1980
H	0.02	0.03	0.03	0.03	0.03	0.03	0.05	0.03	0.03	0.02	0.03	0.03	0.04	Takayanagi and Ozima, 1987
I	0.09	0.10	0.12	0.11	0.11	0.11	0.19	0.13	0.10	0.09	0.11	0.10	0.14	Yiou <i>et al.</i> 1991
J	0.11	0.13	0.15	0.15	0.15	0.15	0.25	0.17	0.13	0.12	0.15	0.14	0.18	Dohnanyi.1972
K	0.11	0.13	0.15	0.15	0.15	0.15	0.25	0.17	0.13	0.12	0.15	0.14	0.18	Hammer and Maurette, 1996
L	0.14	0.16	0.19	0.18	0.18	0.18	0.31	0.21	0.16	0.14	0.19	0.17	0.22	Peng and Lui 1989

490